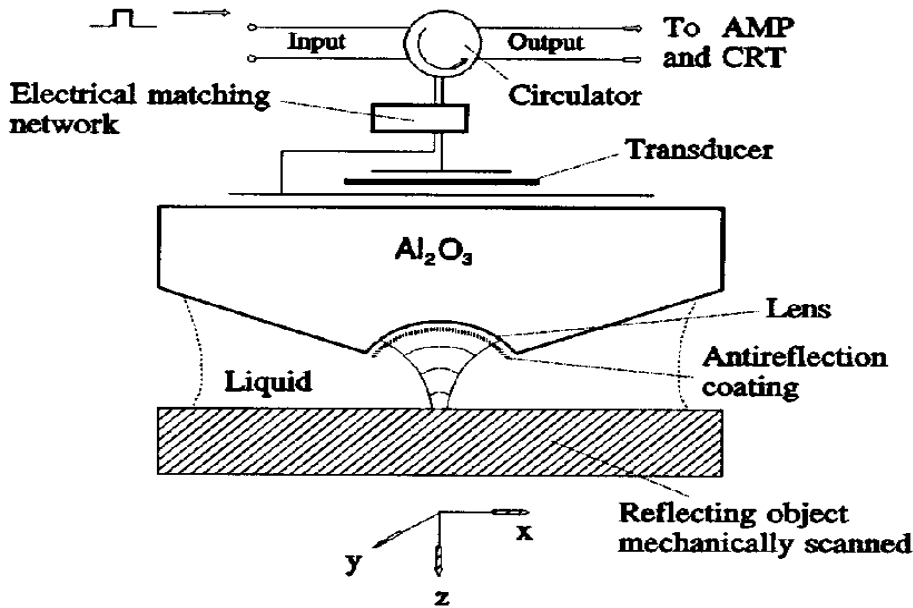


ATOMIC FORCE ACOUSTIC MICROSCOPY (AFAM): AN EXAMPLE OF FORCE MODULATION MICROSCOPY

- Acoustic Microscopy
- Acoustic Microscopy in Surface/ Subsurface Imaging
- Acoustic Microscopy in NonDestructive Evaluation and Characterization (NDEC) of Materials
- Atomic Force Acoustic Microscopy (AFAM)
- AFAM Imaging of Materials Surface
- AFAM Techniques for NDEC of Materials at the Microscopic Scales
- Bibliography

Acoustic Microscopy in Surface/ Subsurface Imaging

reflection- mode Scanning Acoustic Microscope (SAM)



details

- Which is the physical probe?

Elastic (acoustic) beam

- Which is the physical mechanism of image formation?

Recovery of complex elastic waves reflected by a small region of the specimen, scanning over the surface of the specimen

- Which is the source of image contrast?

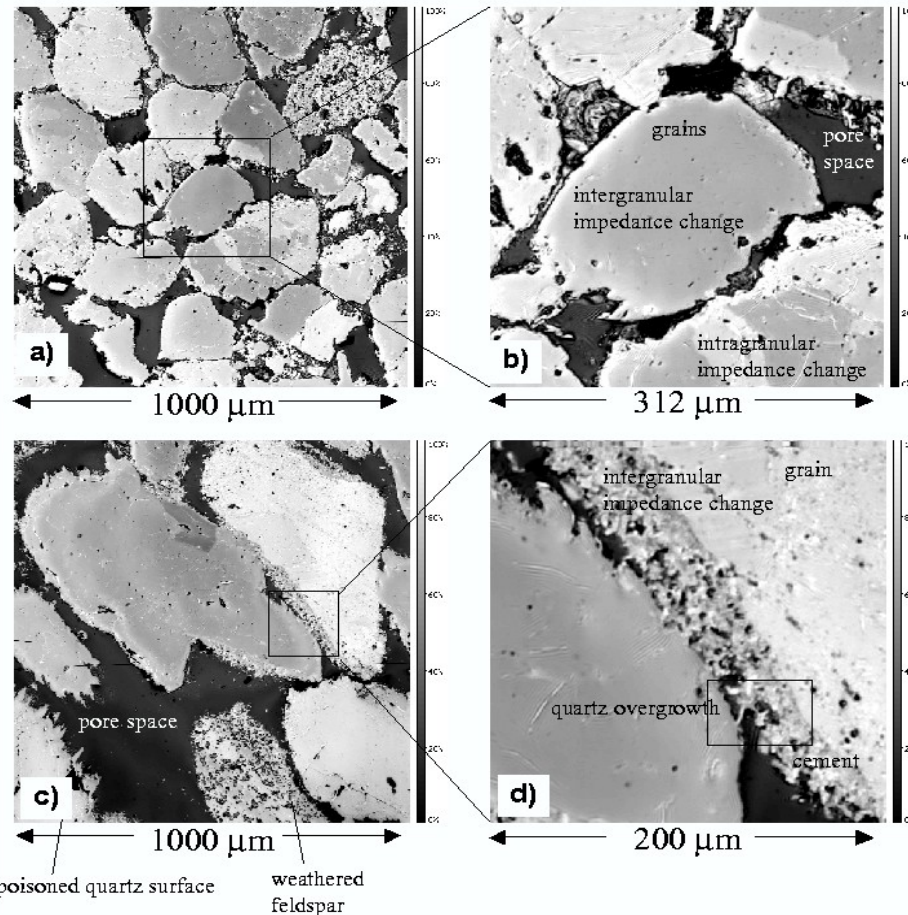
Surface micro- mechanical hetero-structures or local changes of mechanical properties

- Which is the physical mechanism at the basis of information content of reflected waves by the surface?

Complex interference patterns between different components of the reflected elastic beam, due to surface wave excitation into the specimen

Acoustic Microscopy in Surface/ Subsurface Imaging

M. Prasad,
Mapping impedance microstructures in rocks with acoustic microscopy,
The Leading Edge 20, 172-179 (2001).

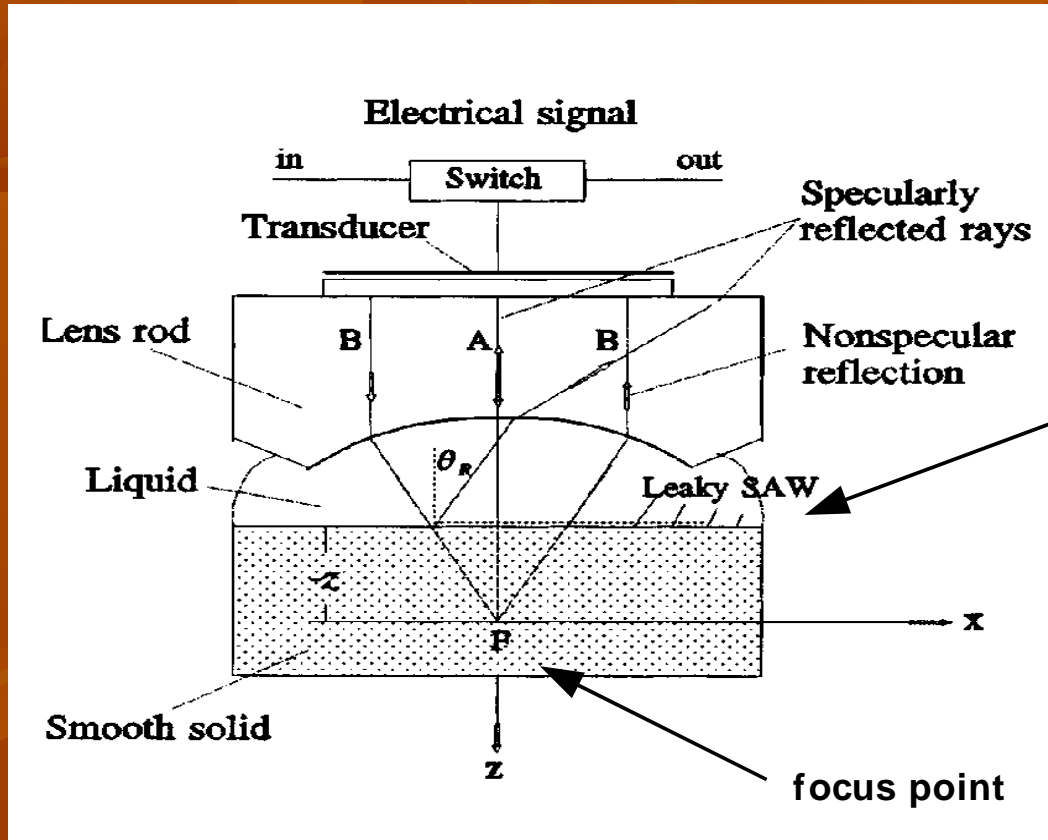


“quantify”
micro-
structures as
variations in
acoustic
impedances!

Figure 7. C-scans of Berea (a, b) and Boise (c, d) sandstones at different magnifications made at 1 GHz. Impedance is gray color-coded: white = high, black = low impedance according to the calibration in Figure 6. The images show various quartz and feldspar grains and the contact areas between them. The black areas are pore spaces; grains are gray. In Berea sandstone (a, b), the grains appear rounded; quartz grains do not show many overgrowths. Between adjacent grains, there is often a layer of cement with lower impedance (see detailed image in b). In Boise sandstone (c, d), quartz grains show typical “poisoned” surfaces, where overgrowths occur in fingers. The contact region between adjacent grains has numerous growths bridging the grains. The box in (d) shows an example of bridging cement between grains. Altered feldspar grains are recognized by strong intragranular impedance variations due to alteration and twinning effects.

Acoustic Microscopy in NonDestructive Evaluation and Characterization of Materials

How can SAM measurements characterize materials surface ?



- The Acoustic Microscope beam can excite Surface Acoustic Waves (SAWs) into the surface of the specimen.
- The SAWs generate leaky (evanescent) surface waves which constitute part of the reflected beam and depend upon material surface properties
- Interference effects between these waves and specularly reflected waves carry information about specimen material properties!

V(z) Analysis: fixed position for the lens- object in the scanning X- Y plane, moving the object out of the focal point, along the Z axis. The recovered signal V(z) contains information about the specimen.

Z is called “defocus distance”

Atomic Force Acoustic Microscopy (AFAM): a new kind of Acoustic Microscopy

SAM imaging and surface materials characterization is limited by resolution:

$$R \approx 0.5 * \lambda_{\text{liquid}}$$

How to improve resolution in acoustic imaging and micro-mechanical characterization?

- **scanning laser acoustic microscopy: various optical schemes for detection of displacements due to surface, longitudinal and shear elastic waves; Abbe's principle implies a resolution not better than λ !**
- **STM techniques for detection of SAWs**
- **Elasticity mapping by AFM in non-contact mode (non-contact scanning force microscopy), at frequencies well below the resonance frequencies of the cantilever (limitations in frequency range - - > limitations in mechanical features characterization!)**

ultrasound waves detection by AFM in contact/ constant force mode

Atomic Force Acoustic Microscopy (AFAM)

Micro- analysis of the AFAM:

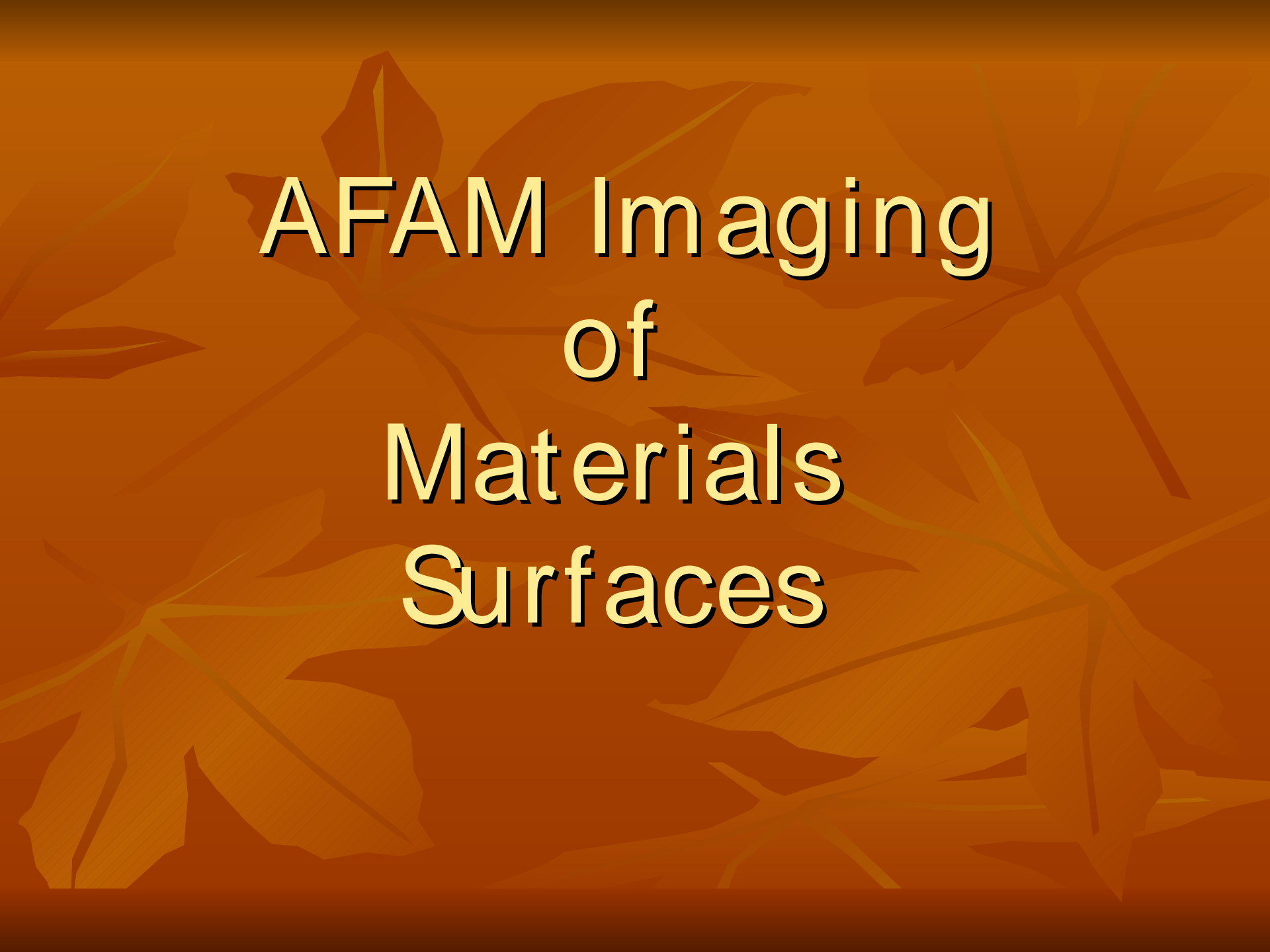
- At ultrasound frequencies, the scanned surface area is smaller than the λ ($\lambda \simeq 0.15\text{-}0.3$ mm at 20 Mhz) so all parts of the surface region can be thought to move uniformly with the same phase and amplitude.
- Changes in the detected amplitude (with the scanning point) are caused by a change of the coupling between the surface and the tip of the AFM
- The local differences in the coupling can be due to micro-geometry of the surface, local changes in the elastic or chemical surface properties or even layers of adsorbate not well bound to the surface.



high sensitivity to microstructures - - > high resolution imaging



non- destructive characterization of surface and subsurface micro-mechanical properties



AFAM Imaging of Materials Surfaces

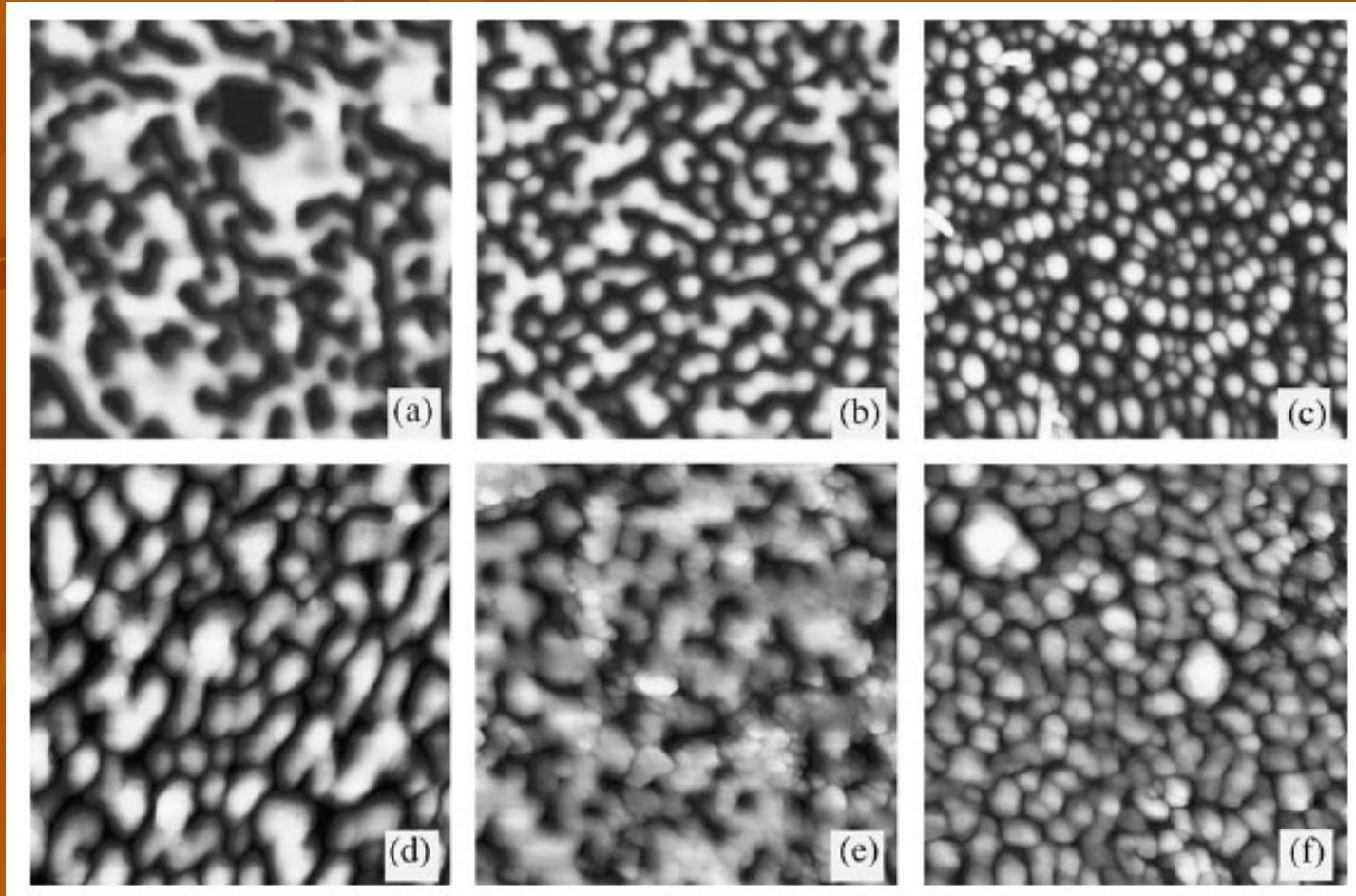
Nanoscale imaging of elastic and piezoelectric properties of nanocrystalline lead calcium titanate

AFAM → can be applied in order to visualize ferroelectric domain patterns, even when the domains are not visible in the topography image.

AFM + AFAM → it is relatively easy to distinguish between the amorphous and the crystalline phase in thin-film PTC samples.

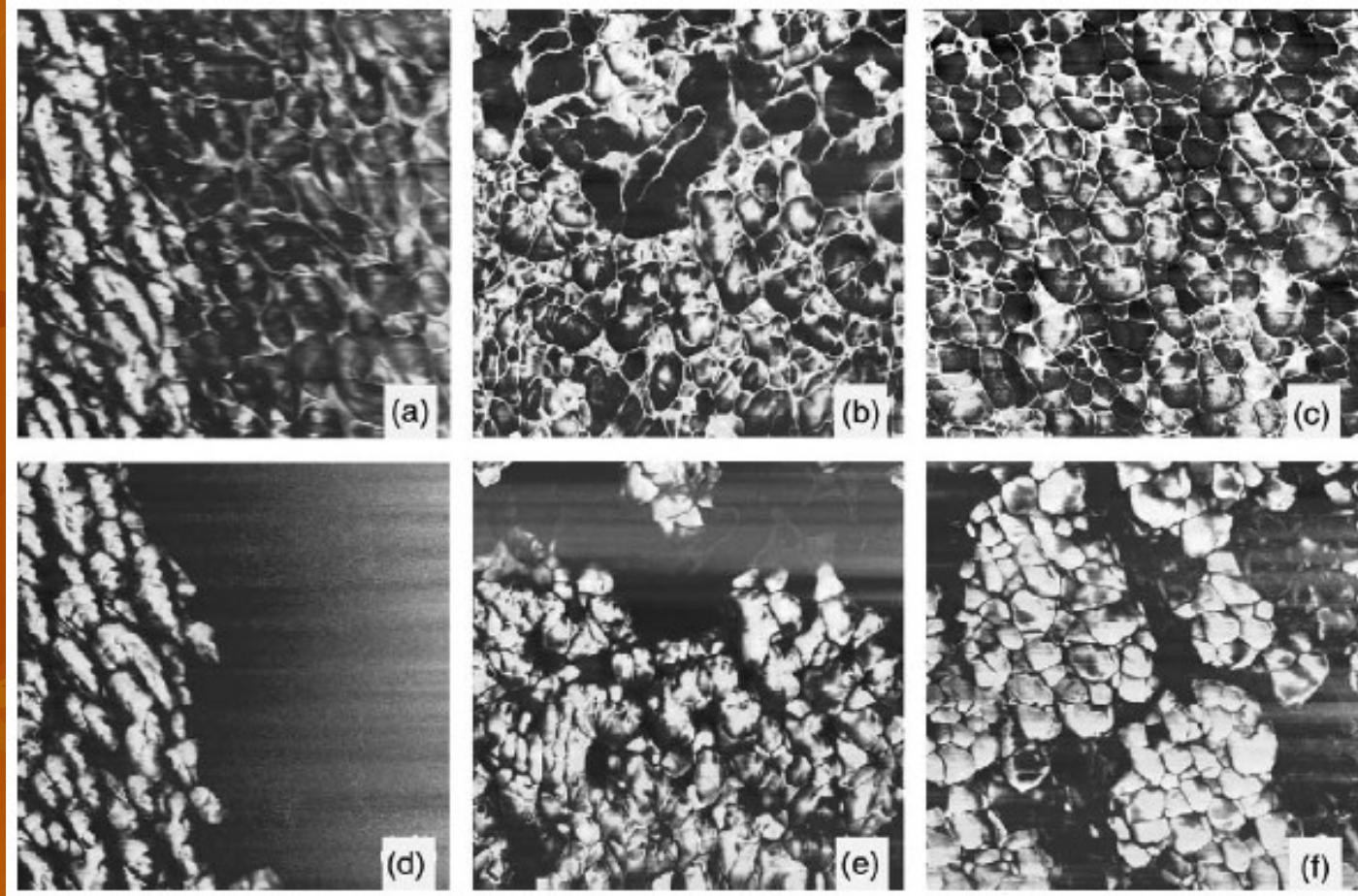
Kopycinska M., Ziebert C., Schmitt H., Rabe U., Hirsekorn S., Arnold W.,
Nanoscale imaging of elastic and piezoelectric properties of nanocrystalline lead calcium titanate. Surface Science 532–535 (2003) 450–455

Nanoscale imaging of elastic and piezoelectric properties of nanocrystalline lead calcium titanate



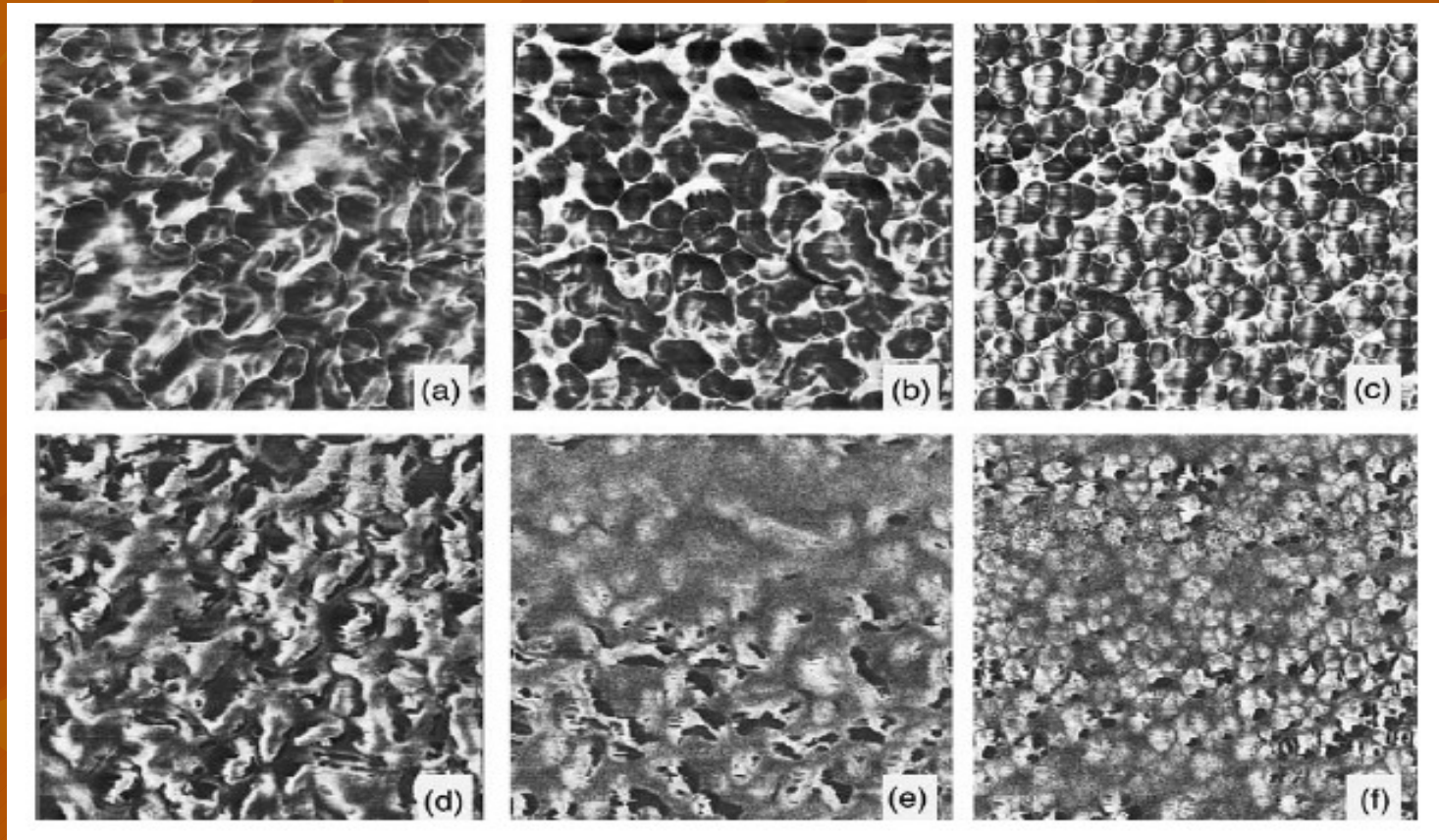
Tapping- mode images of an amorphous thin- film PTC sample (a) and samples annealed at 673 (b), 773 (c), 823 (d), 873 (e), and 923 K (f), respectively. Image size 2x2 μm .

Nanoscale imaging of elastic and piezoelectric properties of nanocrystalline lead calcium titanate



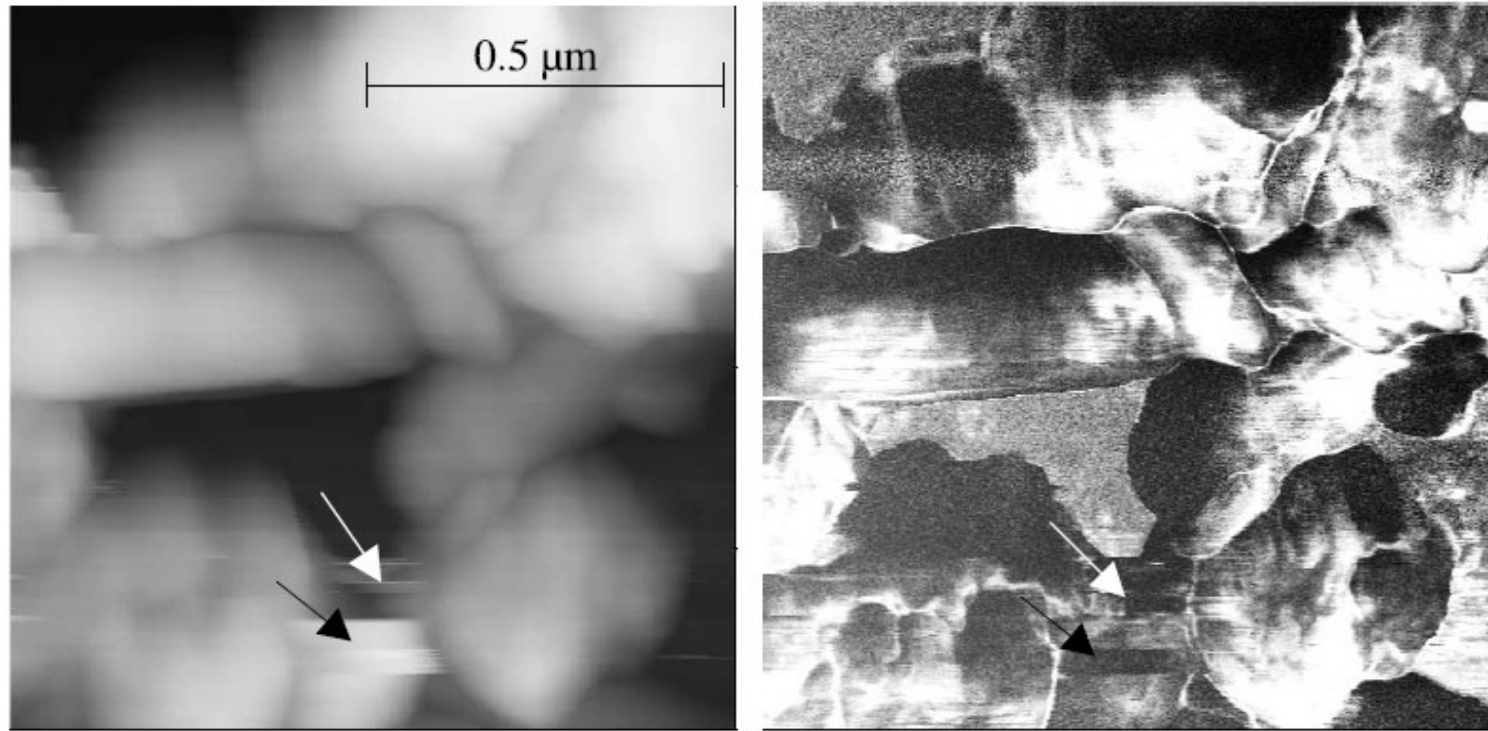
AFAM and ultrasonic piezo-mode images of thin-film PTC samples annealed at 823 K (a and d), at 873 K (b and e) and at 923 K (c and f), respectively. In the upper row the AFAM images are displayed. The lower row presents the corresponding ultrasonic piezomode images. Image size 2 X2 μm

Nanoscale imaging of elastic and piezoelectric properties of nanocrystalline lead calcium titanate



AFAM and ultrasonic piezo- mode images of an amorphous thin- film PTC sample (a and d), and samples annealed at 673 K (b and e) and 773 K (c and f), respectively. In the upper row the AFAM images are displayed. The lower row presents the corresponding ultrasonic piezo- mode images. Image size $2 \times 2 \mu\text{m}$

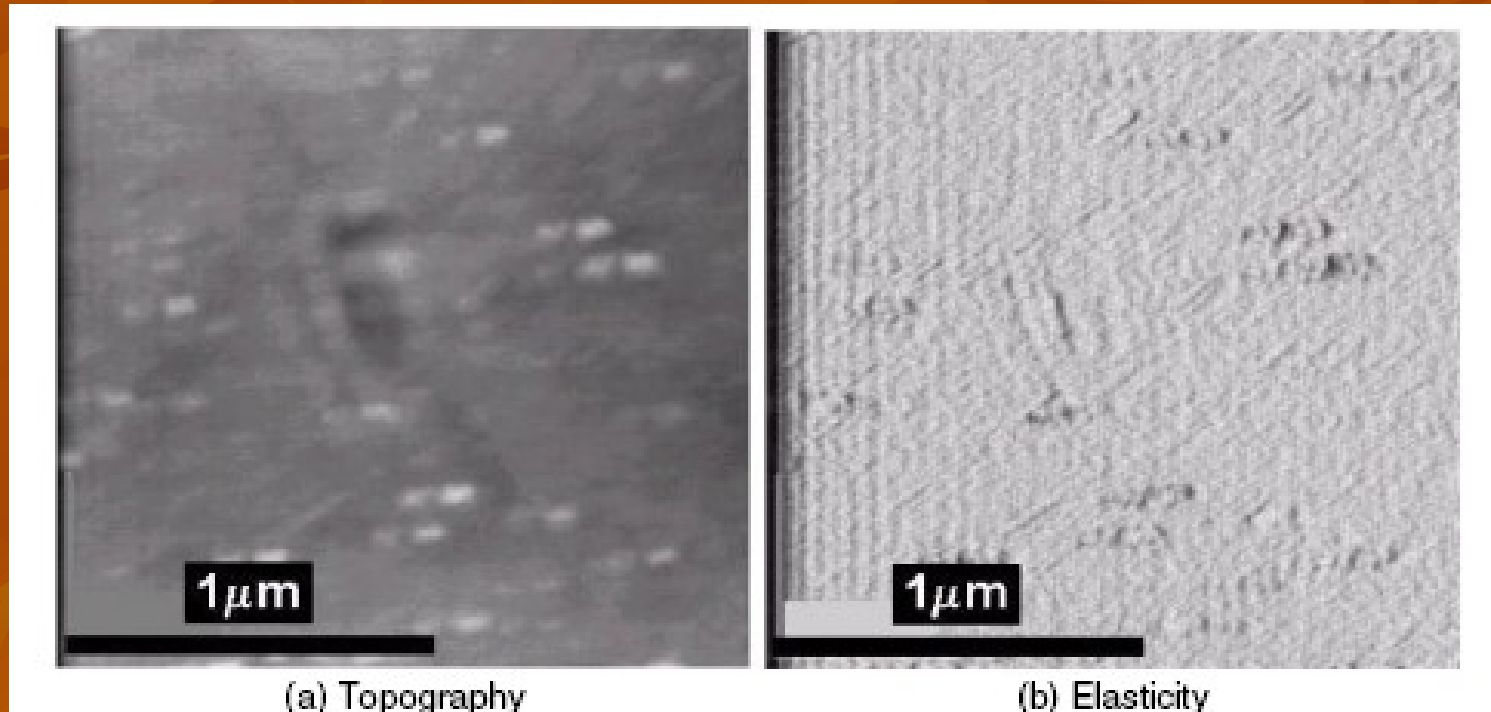
Clay



(a) Topography image, scale 500 nm (b) AFAM image at 987 kHz

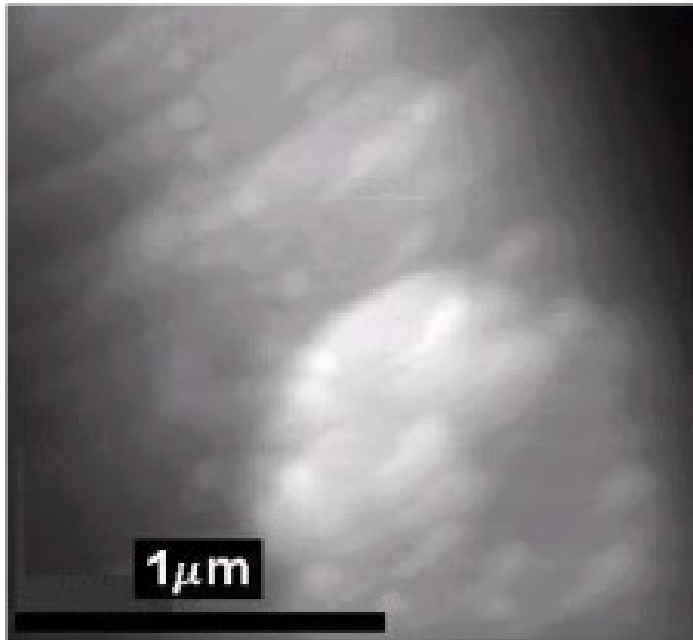
Contact mode AFM of image of dickite powder showing mineral texture (left image). Topography variations, color coded are below 500 nm. The right- side image is an acoustic image with AFAM: It is made with contact mode AFM after insonifying the sample at a resonance frequency of the sample- tip system. Although, topographic effects are small, the AFAM image has some noise and disturbances marked by arrows probably due to sample movements on the glass slide

Sensitivity- enhanced atomic force acoustic microscopy with concentrated- mass cantilevers

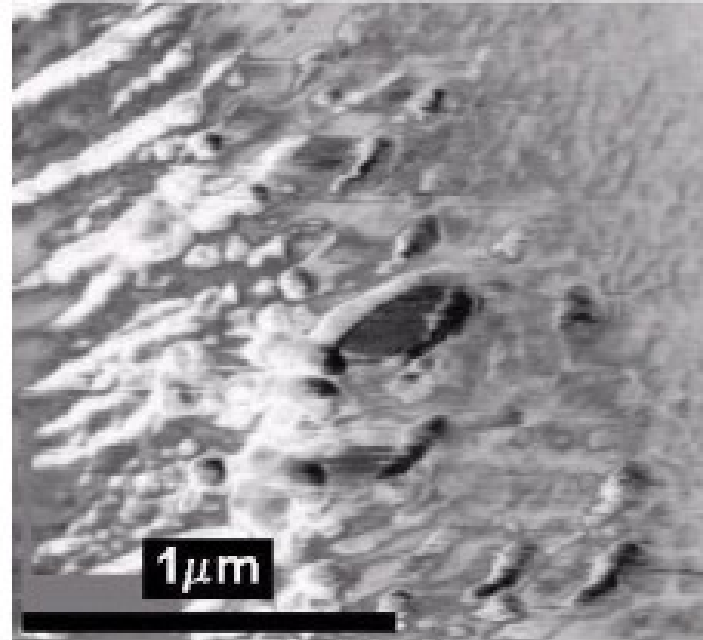


AFAM images of the glass slide surface in the case of the normal cantilever with a W_2C -coated tip

Sensitivity- enhanced atomic force acoustic microscopy with concentrated- mass cantilevers



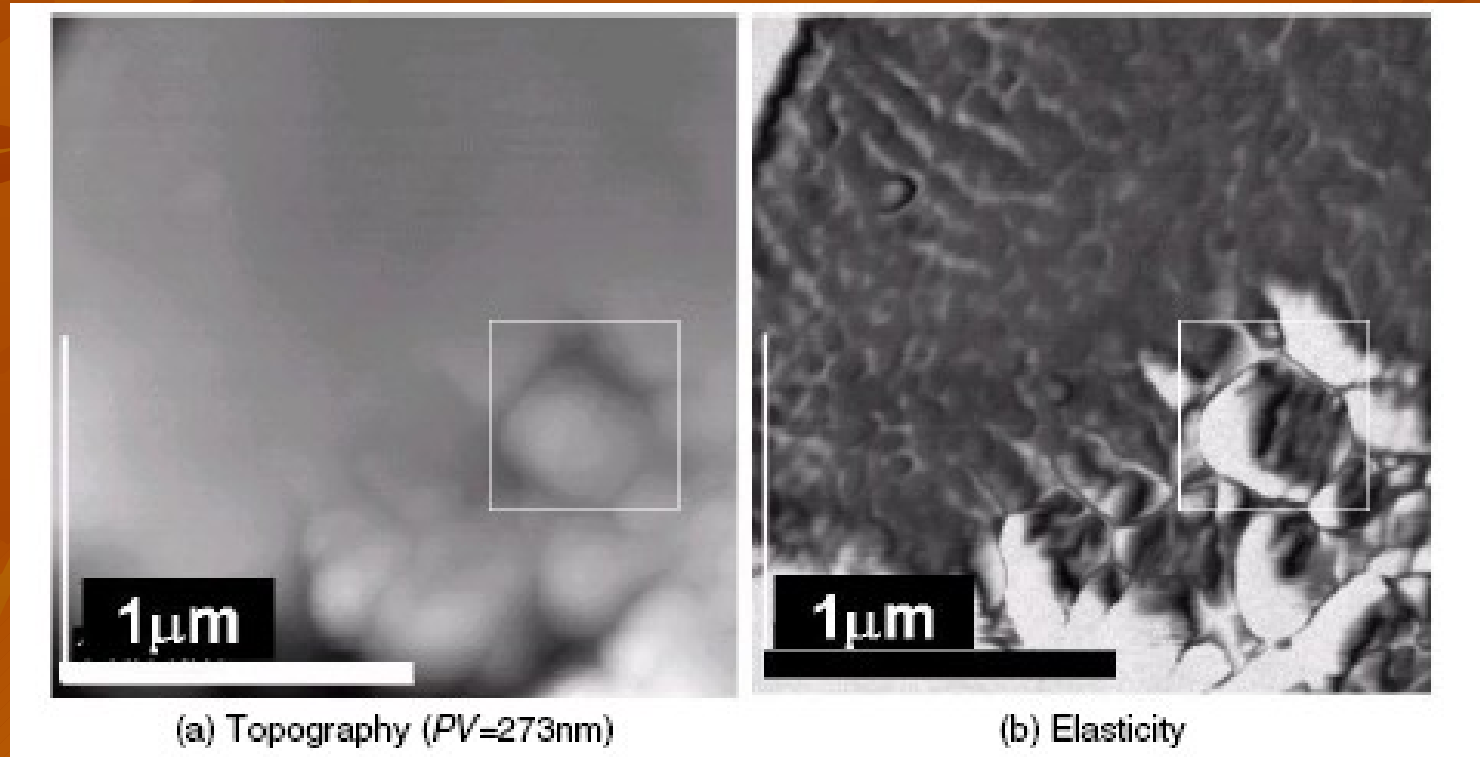
(a) Topography ($PV=350\text{nm}$)



(b) Elasticity

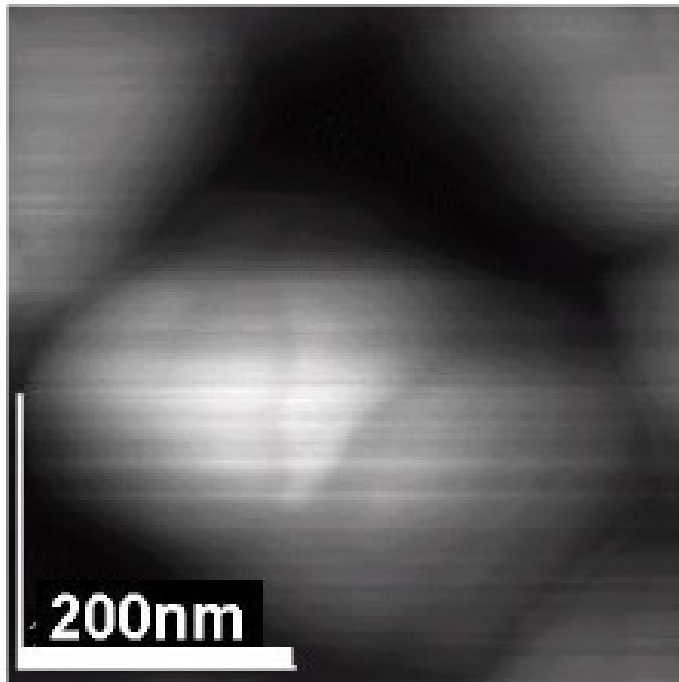
AFAM images of the glass slide surface in the case of the CM cantilever with a W_2C - coated tip

Sensitivity- enhanced atomic force acoustic microscopy with concentrated- mass cantilevers

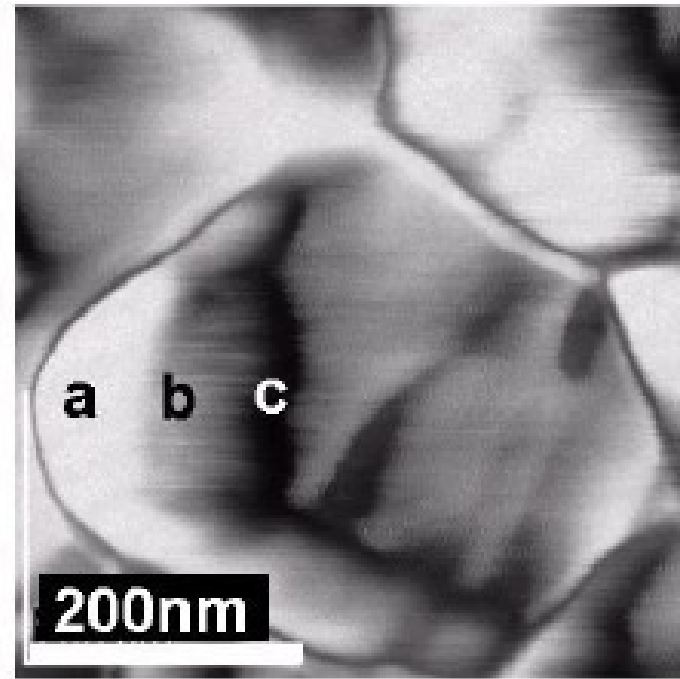


AFAM images of a Ti sheet (as received) in the case of the CM cantilever with a Ti/ Pt- coated flat tip

Sensitivity- enhanced atomic force acoustic microscopy with concentrated- mass cantilevers



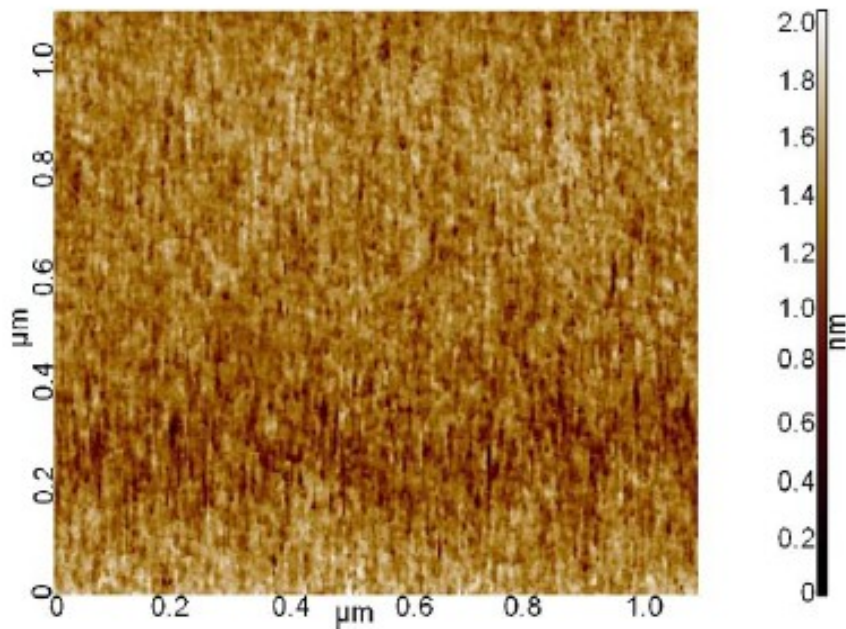
(a) Topography ($PV=64\text{nm}$)



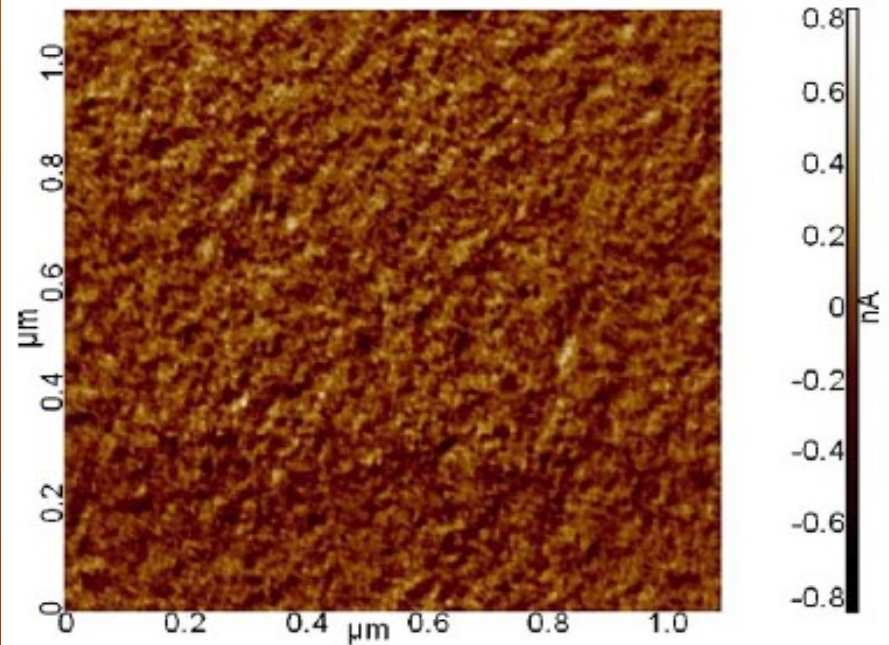
(b) Elasticity

Study the near-surface nanomechanical properties and the surface morphology of hydrogenated amorphous carbon thin film

Topographic image of a- C:H (Vb= -40 V) acquired during an AFAM scan



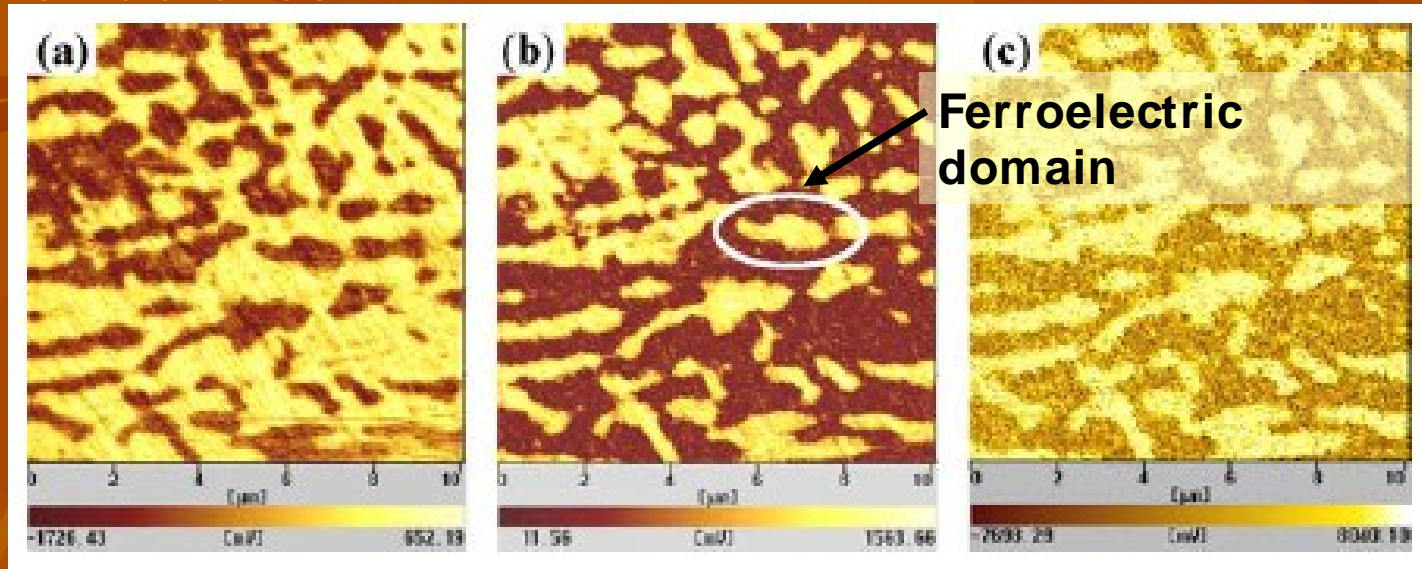
Acoustic image of a- C:H (Vb= -40 V) acquired during an AFAM scan



The elastic properties of the surface are represented through the amplitude variation. The darker regions in the image correspond to lower contact stiffness and as a consequence to lower E_f values

Local elasticity imaging of ferroelectric domains by low-frequency atomic force acoustic microscopy

- Acoustic imaging mechanism of domain structures

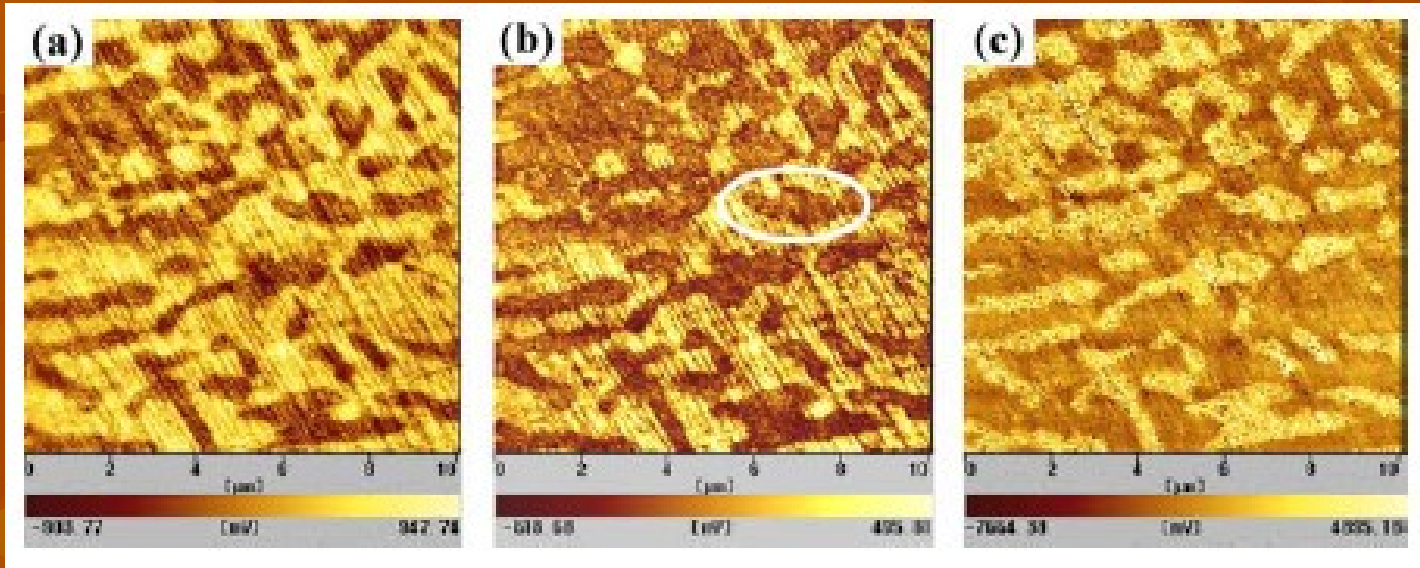


The acoustic image (a), amplitude image (b) and phase image (c) of (001)- oriented PMN-33%PT single by atomic force microscopy at the frequency of 2.9 kHz.



Local elasticity imaging of ferroelectric domains by low-frequency atomic force acoustic microscopy

- Local contact stiffness of domain structures



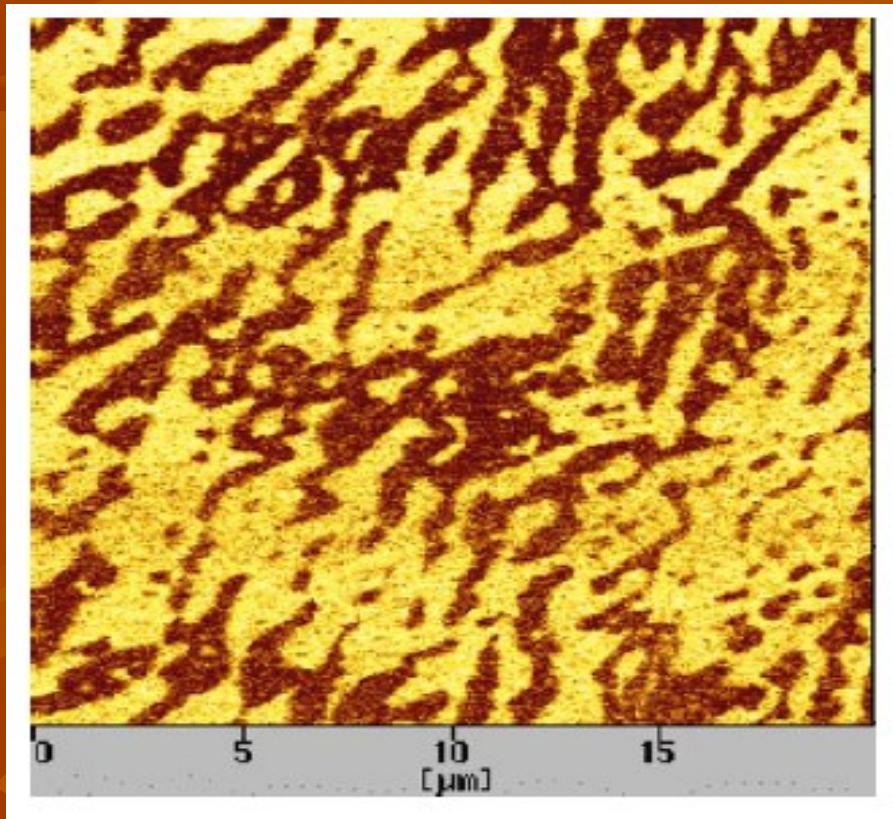
Piezoresponse of the ferroelectric domain

The piezoresponse image (a), amplitude image (b) and phase image (c) of domain structures in (001)- oriented PMN–33% PT single



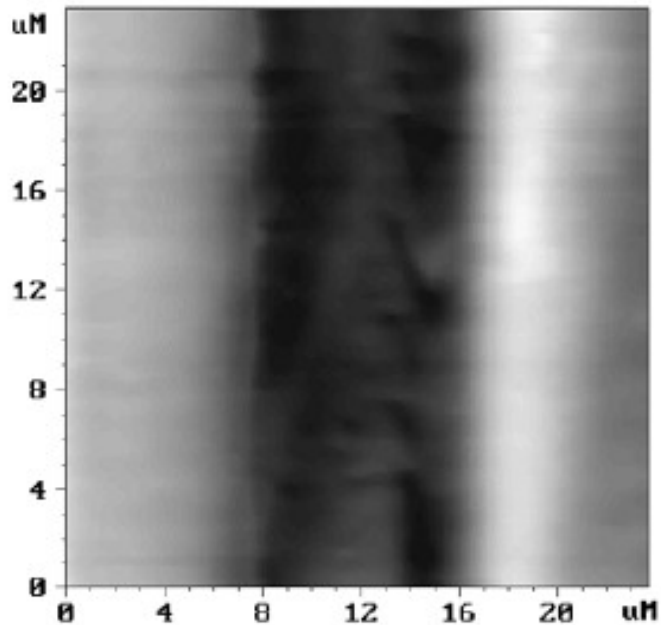
Local elasticity imaging of ferroelectric domains by low-frequency atomic force acoustic microscopy

- Local contact stiffness of domain structures

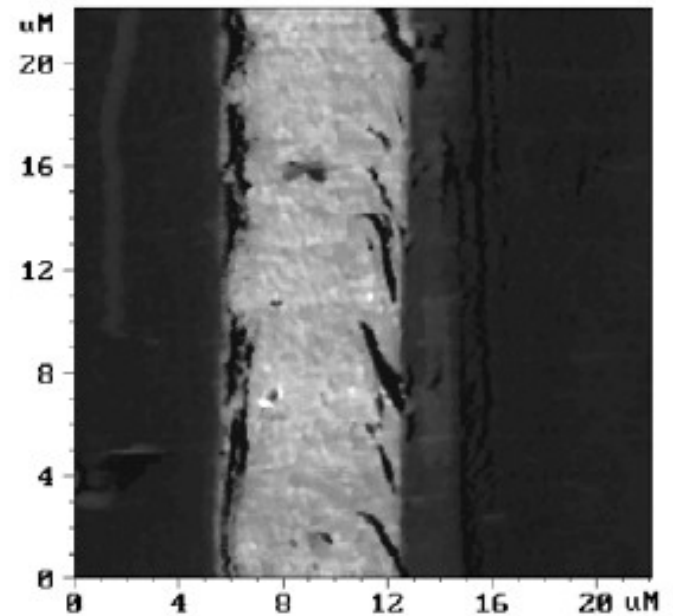


The piezoresponse image of domain structures in another scanning area of (001)-oriented PMN-33% PT single

Atomic Force Acoustic Microscopy as a tool for polymer elasticity analysis



a



b

Contact mode topography (a) and AFAM (b) image of polyethylene sample cross-section with stripes of different density

Ultrasonic Force Microscopy (UFM)

The Ultrasonic Force Microscopy (UFM) technique consists in vibrating the sample at frequencies much higher than the resonant frequency of the cantilever and measuring the deflection and/or torsional vibration of the cantilever that is much softer than the tip-sample contact rigidity.

It gives nanometer resolution elastic or subsurface images, and moreover, discriminates features of different elastic properties, by controlling the direction of vibration forces.

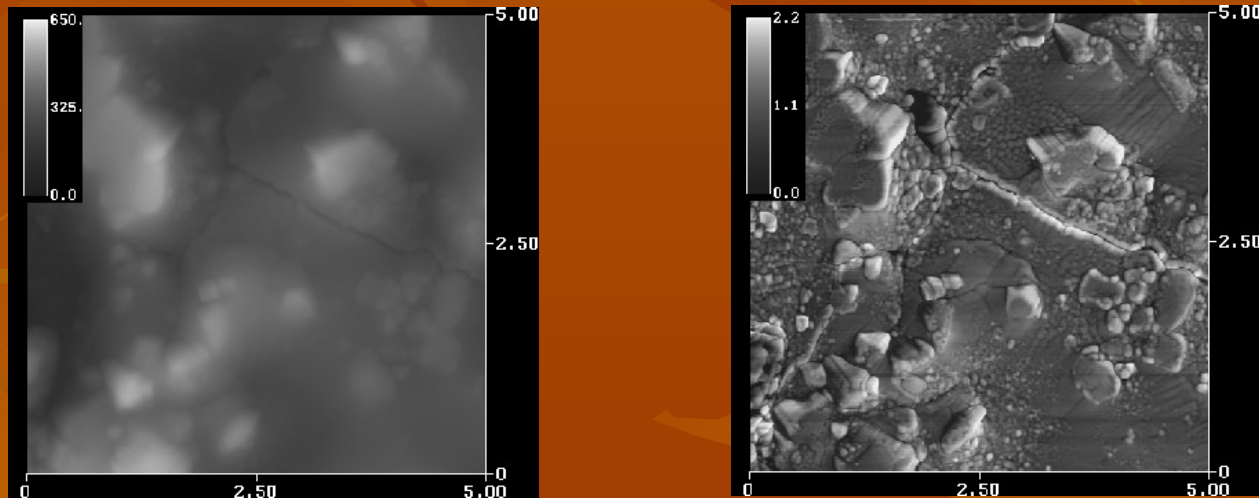


Fig.1: This figure is a 5 micron scan of a laser-modified surface on Al_2O_3 -TiC. An AFM surface topography image is on the left with a UFM amplitude image on the right. Material changes from micro and nano-cracks, loosened grains, surface ripples, twinned grains and nano droplet features are seen with greater detail in the UFM image.

The model

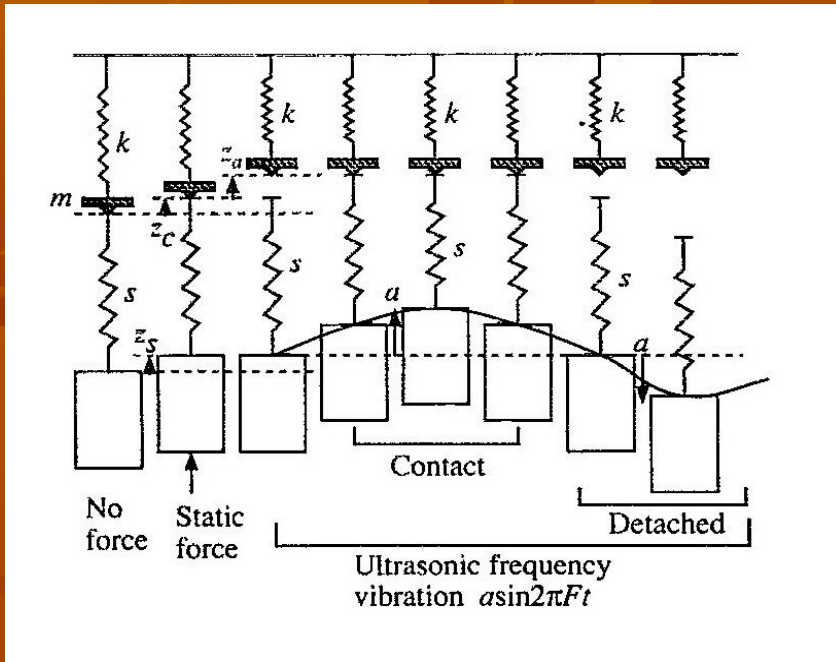


Fig.2: Model of the tip- sample system

z_c : cantilever displacement due to repulsive force

z_a : cantilever deflection due to the vibration

s : spring constant of the tip- sample contact rigidity

k : cantilever spring constant

a : sample vibration amplitude

The system tip- sample is represented by two masses connected with two springs with elastic constant s (sample) and k (tip). The coupling of the two systems depends on the amplitude and the frequency of the vibration of the sample.

If the sample vibrates at a frequency F lower than the cantilever resonant frequency F_0 , the cantilever also vibrates following the sample vibration. If s is approximated by a linear spring, the peak-to-peak cantilever vibration amplitude is given by:

$$V = 2z_c \frac{a/z_c}{1 + k/s}$$

and V does not significantly depend upon the spring constant ratio k/s , if it is varied from 10^{-1} to 10^{-4} (see Fig.3)

When the sample vibrates at ultrasonic frequencies, much higher than the cantilever resonant frequency ($F \gg F_0$), the cantilever cannot follow the sample vibration. When the vibration amplitude exceeds the initial sample compression, the tip is detached from the sample for a certain period within one vibration cycle.

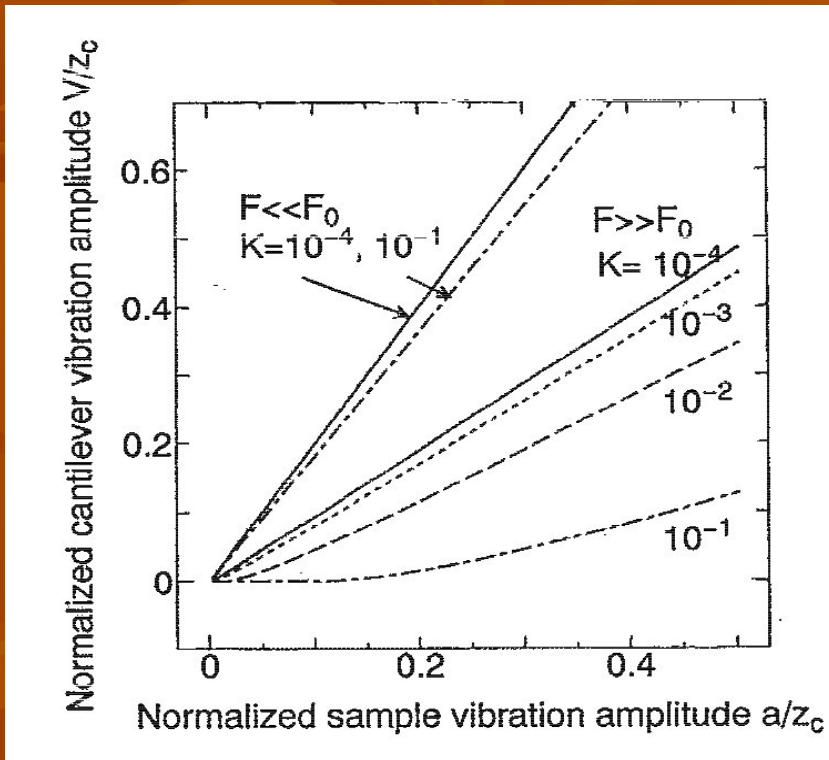


Fig.3: Calculated cantilever vibration amplitude in the low-frequency vertical force modulation mode ($F \ll F_0$) and the cantilever deflection in the vertical UFM mode ($F \gg F_0$).

During the contact, a repulsive force is acted and the tip is indented into the sample even when the sample is much more rigid than the cantilever [Fig.4(b)]. If the time dependence of sample vibration is approximated by a triangular function, the averaged repulsive force for one cycle is:

$$F_m = \frac{s}{4a} \left(\frac{k}{s} z_c + a - z_a \right)^2$$

and, being the cantilever restoring force:

$$F_m = k \left(z_c + z_a \right)$$

it is possible to obtain $z_a(a)$:

$$z_a = z_c \left[\frac{k}{s} + \frac{a}{z_c} + 2 \frac{ka}{s z_c} - 2 \sqrt{\frac{ka}{s z_c} \left(\frac{k}{s} + 1 \right) \left(\frac{a}{z_c} + 1 \right)} \right]$$

The experiment

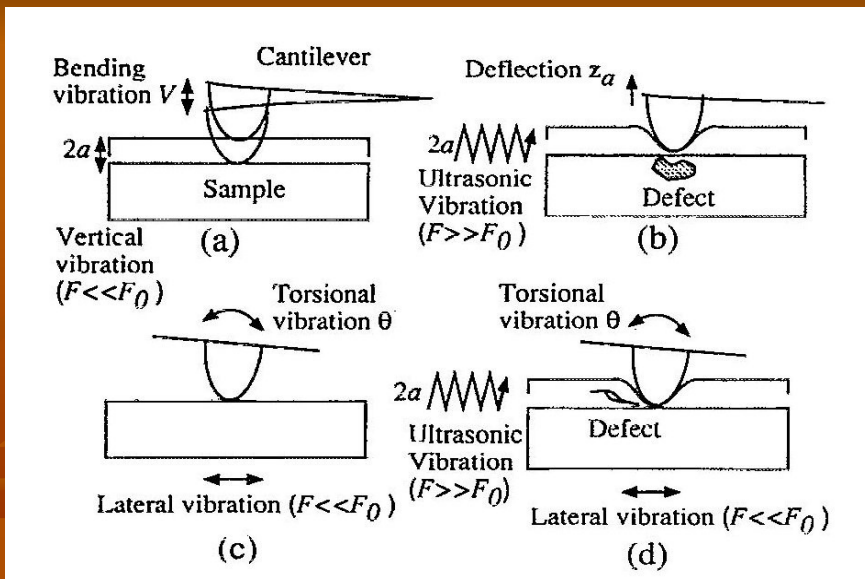


Fig. 3: Imaging schemes of the force modulation modes in AFM and ultrasonic force microscopy.

- (a) vertical force modulation mode,
- (b) vertical UFM mode,
- (c) lateral force modulation mode,
- (d) lateral UFM mode.

When the sample is laterally vibrated at frequencies lower than the cantilever resonance, torsional vibration of the cantilever is excited by the surface friction force as illustrated in Fig. 3(c), (lateral force modulation).

If additional vertical ultrasonic vibration of the sample is excited, the torsion torque of the cantilever is changed during the tip is tilted. This torque is sensitive not only to the surface friction, but also to the subsurface shear rigidity, because it is generated during the tip is indented into the sample. Therefore, subsurface features such as a delamination or an edge dislocation that modify the shear rigidity would be imaged by measuring the torsional vibration [Fig. 3(d)].

It is measured z_a by modulating the vibration amplitude and measuring the cantilever deflection vibration at the modulation frequency. If there is no feedback the peak-to-peak cantilever vibration amplitude is $V = z_a$. Thus it is possible to obtain images representing the elastic property [Fig. 3(b)].

Sometimes, the sample position is feedback controlled to suppress the cantilever deflection fluctuation in frequencies much lower than the modulation frequency. This procedure enables to obtain a simultaneous approximate topography image and to avoid tip crashing to the sample during the scanning.

Bibliography

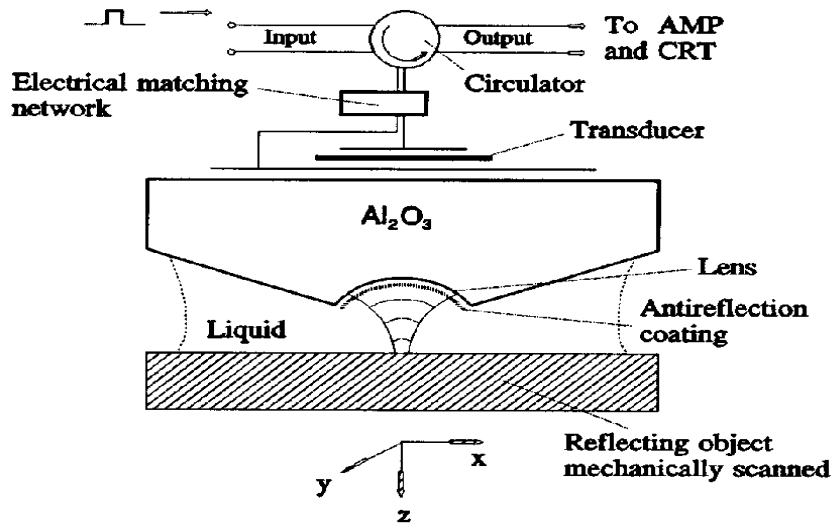
- Z. Yu, S. Borek, *Scanning acoustic microscopy and its applications to material characterization*, Rev. Mod. Phys. 67, 836- 891 (1995) ([article.pdf](#))
- M. Prasad, *Mapping impedance microstructure in rocks with acoustic microscopy*, The Leading Edge 20, 172- 179 (2001) ([article.pdf](#))
- U. Rabe, W. Arnold, *Acoustic microscopy by atomic force microscopy*, App. Phys. Lett. 64,1493- 1495 (1994) ([article.pdf](#))
- U. Rabe, S. Amelio, E. Kester, V. Scherer, S. Hirsekorn, W. Arnold, *Quantitative determination of contact stiffness using atomic force acoustic microscopy*, Ultrasonics 38, 430- 437 (2000) ([article.pdf](#))
- Kopycinska M., Rabe U., Arnold W. and Prasad M. *Measurement of Young's modulus of clay minerals using atomic force acoustic microscopy*. Geophysical Research Letters, 29, N°. 8, 10.1029/ 2001 GL014054, 2002 ([article.pdf](#))

Bibliography

- Kopycinska M., Ziebert C., Schmitt H., Rabe U., Hirsekorn S., Arnold W., *Nanoscale imaging of elastic and piezoelectric properties of nanocrystalline lead calcium titanate*. Surface Science 532–535 (2003) 450–455 ([article.pdf](#))
- Muraoka M., *Sensitivity-enhanced atomic force acoustic microscopy with concentrated-mass cantilevers*. Nanotechnology 16 (2005) 542–550 ([article.pdf](#))
- Kassavetis S.N., Logothetidis S., Matenoglou G.M., *Near-surface mechanical properties and surface morphology of hydrogenated amorphous carbon thin films*. Surface & Coatings Technology 200 (2006) 6400–6404 ([article.pdf](#))
- Zeng H.R., Yu H.F., Hui S.X., Chu R.Q., Li G.R., Luo H.S., Yin Q.R. *Local elasticity imaging of ferroelectric domains in $Pb(Mg_{1/3}Nb_{2/3})O_3$ - $PbTiO_3$ single crystals by low-frequency atomic force acoustic*. Solid State Communications 133 (2005) 521–525 ([article.pdf](#))
- Efimov A.E., Saunin S.A. *Atomic Force Acoustic Microscopy as a tool for polymer elasticity analysis*, SPM- 2002, Proceedings, 79. ([article.pdf](#))
- Yamanaka K., Ogiso H., Kolosov O., *Ultrasonic force microscopy for nanometer resolution subsurface imaging*, Applied Physics Letters, 84 (2), 178- 180 (1994) ([article.pdf](#))

Acoustic Microscopy in Surface/ Subsurface Imaging

Reflection- mode SAM in details



- **acoustic lens**: interface between a solid material and a liquid one; the solid material is a rod cut along a specific crystallographic axis; in the center of one face of the rod, a concave spherical surface is ground for obtaining focusing of acoustic waves;
- **transducer in emitter mode**: short (30 ms time window) RF pulse - - > plane acoustic wave propagation in the rod, then focusing on the axis of the lens by refraction at the spherical interface;
- the object to be imaged is placed at the focus of the lens;
- partial reflection at the object- liquid interface - - > echoes are recovered by the same transducer in receiver- mode;
- the object is mechanically scanned, point- by- point - - > image = 2D map of reflectivity pattern.

- spherical aberration as the only source of aberration: very low due to high levels relative refractive index;
- resolution R: diffraction- limited, $R \approx 0.5 * \lambda_{\text{liquid}}$ at high frequencies (0.4 μm at 2.0 GHz; 0.025 μm at 8 GHz with liquid He at 0.1 °K)

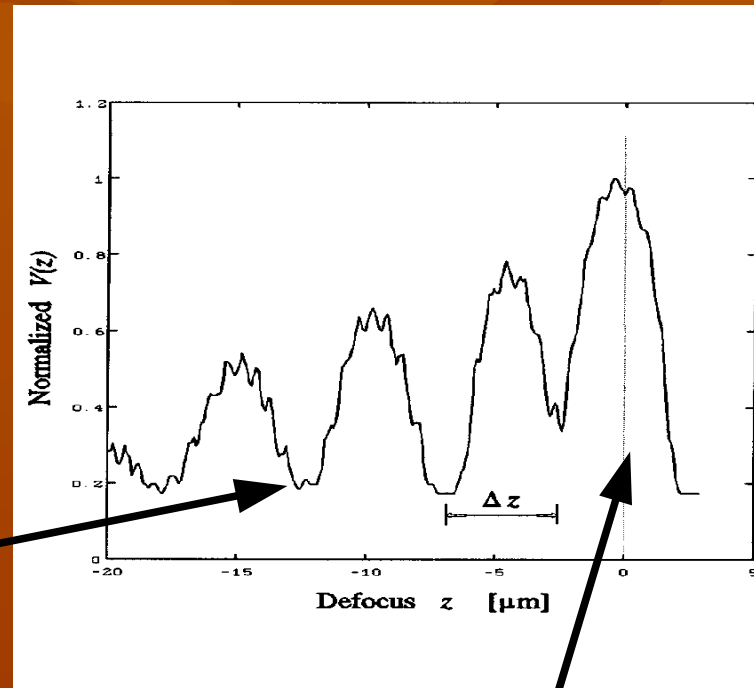
- subsurface imaging due to penetration depth of Surface Acoustic Waves (SAWs) generated along the interface between liquid and object;
- penetration ability: trade- off between resolution and penetration at high frequencies (Kelvin- Voigt model of attenuation, $\propto \nu^2$)

[Back to the general description of SAM](#)

Acoustic Microscopy in NonDestructive Evaluation and Characterization of Materials: the $V(z)$ Analysis. #1

$V(z)$ Analysis: fixed position for the lens- object in the scanning X- Y plane, moving the object out of the focal point, along the Z axis. The recovered signal $V(z)$ contains information about the specimen.

Z is called “defocus distance”



interference patterns:
oscillations with period(s) Δz
<--> “acoustic material
signature”

primary (specular)
reflection, defocus = 0

Acoustic Microscopy in NonDestructive Evaluation and Characterization of Materials: the V(z) Analysis, #2

incident beam at critical angle of pure transmission: $\theta_R = \arcsin(v_{\text{liquid}} / v_R)$, from Snell's law

generation of leaky Rayleigh waves: special kind of SAWs

models of interference phenomena

Ray optical model: double-ray interference model

Fourier angular spectrum analysis

Result: indirect measurement of leaky Rayleigh waves velocity

$$V_R = \frac{V_{\text{liquid}}}{[1 - (1 - v_{\text{liquid}} / (2v \Delta z))]^{1/2}}$$

Result: indirect measurement of surface reflectance function $R(\theta)$ (inverse problem)

$$V(z) = \int_0^{\theta_m} P^2(\theta) u_1^2(\theta) R(\theta) \cdot e^{-2ik_{\text{liquid}} z \cos(\theta)} \sin(\theta) \cos(\theta) d\theta$$

- attenuation of SAWs (< - - grain size, porosity, density of micro-cracks, etc. near the surface)
- elastic constants
- mechanical impedances

ATOMIC FORCE ACOUSTIC MICROSCOPY



Yotselys Lopez Gonzalez

Dept. of Chemical Engineering and Materials Sciences

M. Griffa, M. Nobili

Dept. of Physics

Politecnico di Torino

III Level Course: “AFM- STM Techniques for Physics and Engineering”
Lectured by Prof. R. Gonnelli, Dept. of Physics, Politecnico di Torino
2006 edition